Regulation of Ganglioside Biosynthesis by Enzyme Complex Formation of Glycosyltransferases†

Erhard Bieberich,*,‡ Sarah MacKinnon,‡ Jeane Silva,‡ Donna D. Li,‡ Tewin Tencomnao,‡ Louis Irwin,§ Dmitri Kapitonov,|| and Robert K. Yu‡

Institute of Molecular Medicine and Genetics, Medical College of Georgia, Augusta, Georgia 30912, Department of Biological Sciences, University of Texas at El Paso, El Paso, Texas 79968, and Department of Neurosurgery, University of Pennsylvania, Philadelphia, Pennsylvania 19104

Received April 22, 2002; Revised Manuscript Received July 2, 2002

ABSTRACT: Three key regulatory enzymes in ganglioside biosynthesis, sialyltransferase I (ST1), sialyltransferase II (ST2), and *N*-acetylgalactosaminyltransferase I (GalNAcT), have been expressed as fusion proteins with green, yellow, or red fluorescent protein (GFP, YFP, or RFP) in F-11A cells. F-11A cells are a substrain of murine neuroblastoma F-11 cells that contain only low endogenous ST2 and GalNAcT activity. The subcellular localization of the fusion proteins has been determined by fluorescence microscopy, and the ganglioside composition of these cells was analyzed by high-performance thin-layer chromatography (HPTLC). ST2-GFP (85 kDa) shows a distinct Golgi localization, whereas ST1-YFP (85 kDa) and GalNAcT-RFP (115 kDa) are broadly distributed in ER and Golgi. Untransfected F-11A cells contain mainly GM3, whereas stable transfection with ST2 or GalNAcT results in the predominant expression of b-series complex gangliosides (BCGs). This result indicates that the expression of ST2 enhances the activity of endogenous GalNAcT and vice versa. The specificity of this reaction has been verified by in vitro activity assays with detergent-solubilized enzymes, suggesting the formation of an enzyme complex between ST2 and GalNAcT but not with ST1. Complex formation has also been verified by co-immunoprecipitation of ST2-GFP upon transient transfection with GalNAcT-HA-RFP and by GFP-to-RFP FRET signals that are confined to the Golgi. FRET analysis also suggests that ST2-GFP binds tightly to pyrene-labeled GM3 but not to ST1. We hypothesize that an ST2−GM3 complex is associated with GalNAcT, resulting in the enhanced conversion of GM3 to GD3 and BCGs in the Golgi. Taken together, our results support the concept that ganglioside biosynthesis is tightly regulated by the formation of glycosyltransferase complexes in the ER and/or Golgi.

The biosynthesis of glycosphingolipids is catalyzed by a series of ER- and Golgi-resident glycosyltransferases (Figure 1; *2*, *3*). Most recently, it has been shown that two glycosyltransferases participating in ganglioside biosynthesis, *N*-acetylgalactosaminyltransferase I (GalNAcT)[1] and galactosyltransferase II (GalT2), form a Golgi-localized enzyme complex that is stabilized by noncovalent association (*4*). This enzyme association has been suggested to facilitate the biosynthesis sequence from GM3/GD3 to GM1/GD1b via GM2/GD2 as intermediates (*4*). Recently, we have introduced a multienzyme kinetic analysis (MEKA) that predicts a fast transport of gangliosides between glycosyltransferases that catalyze subsequent steps in the biosynthesis sequence (Figure 1; *5*). MEKA is consistent with the enzyme kinetics of a glycosyltransferase complex, the formation of which has been suggested previously (*6*, *7*). MEKA, however, also predicts the efficacy of additional enzyme complexes, in particular, between sialyltransferase II (ST2) and GalNAcT, to facilitate the biosynthesis of b-series complex gangliosides (BCGs) from GM3 (Figure 1). Enhanced biosynthesis of BCGs has been suggested to contribute to the survival of neuronal progenitors in embryonal mouse brain (*8*). Activation of ganglioside biosynthesis by complex formation of glycosyltransferases may sustain a shift from simple gangliosides to BCGs that has been observed during rat and mouse brain development (*3*, *8*).

We identified a substrain of murine neuroblastoma F-11 cells, termed F-11A, that mainly expresses GM3 unless transfected with a construct containing a cDNA encoding ST2 (*8*). Stable transfection with ST2 results in the predominant expression of BCGs, indicating that the activity of endogenous GalNAcT is enhanced, thereby facilitating the synthesis of BCGs from GM3. The cDNA of ST2 used

† Supported by NIH Grant NS 11853 to R.K.Y.

* Address correspondence to this author. Phone: 706-721-9113. Fax: 706-721-8685. E-mail: ebieberich@mail.mcg.edu.

‡ Medical College of Georgia.

§ University of Texas.

|| University of Pennsylvania.

[1] Abbreviations: GalNAcT (GNT), UDP-*N*-acetylgalactosaminyl: GM3/GD3 *N*-acetylgalactosaminyltransferase; HPTLC, high-performance thin-layer chromatography; ST1, CMP-NeuAc:LacCer α2,3-sialyltransferase; ST2, CMP-NeuAc:GM3 α2,8-sialyltransferase; GFP, green fluorescent protein; RFP, red fluorescent protein; YFP, yellow fluorescent protein; BCGs, b-series complex gangliosides; FRET, fluorescence resonance energy transfer; endo H, endoglucosamindase H; glyco F, glycopeptidase F; HA, hemagglutinin. Other glycosphingolipid structures are abbreviated according to the IUPAC−IUB recommendation (IUPAC−IUB Commission on Biochemical Nomenclature, 1977) except gangliosides, which are abbreviated according to Svennerholm (*1*).

10.1021/bi0259958 CCC: $22.00
Published on Web 08/30/2002

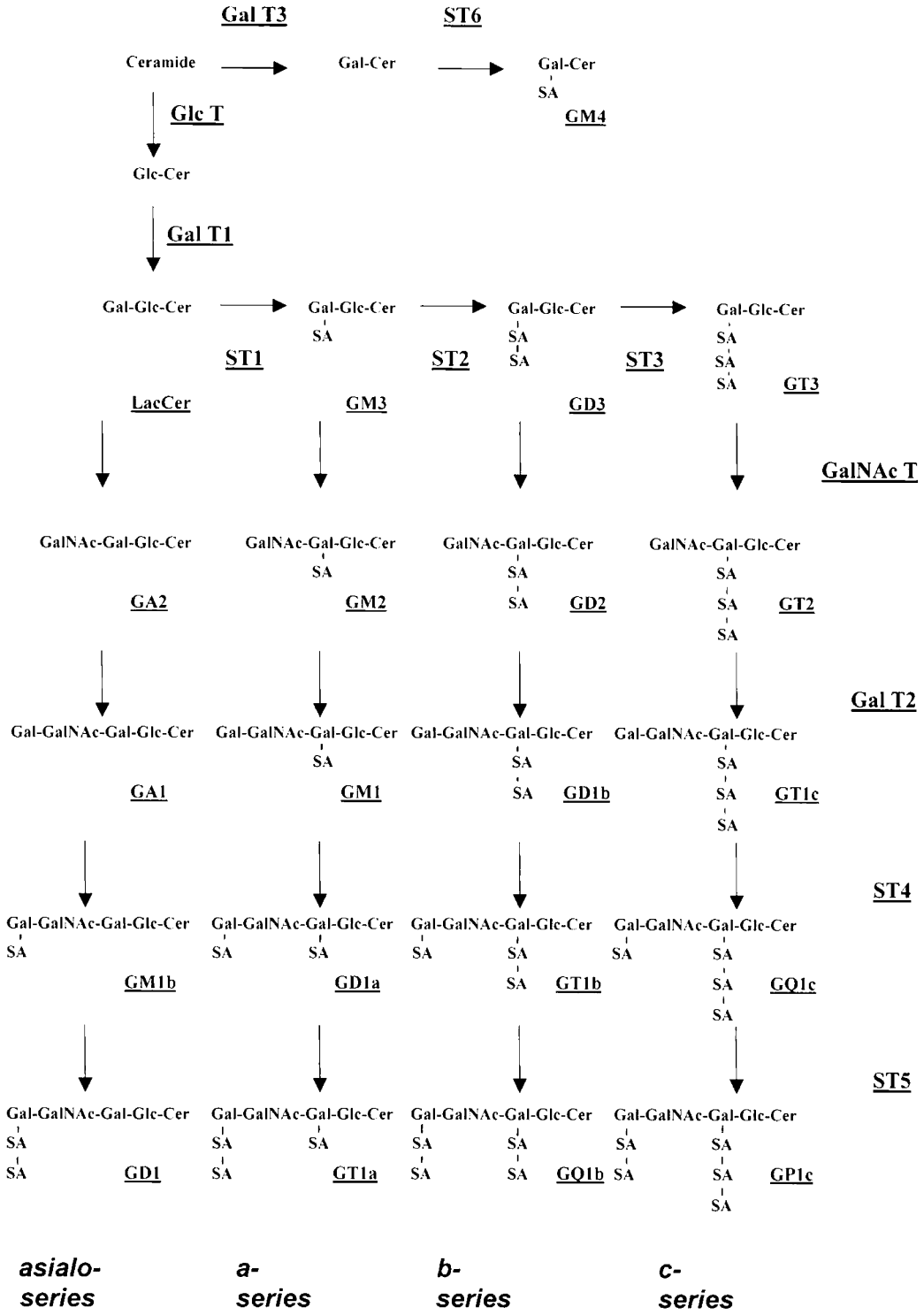

FIGURE 1: Pathways of ganglioside biosynthesis.

for stable transfection of F-11A cells was endowed with the sequence of the FLAG epitope and green fluorescent protein (ST2-FLAG-GFP). Untransfected F-11A or ST2-FLAG-GFP transfected cells were also used for transfection with ST1 or GalNAcT, the cDNAs of which were endowed with the sequences of the hemagglutinin (HA) epitope and/or red fluorescent protein (ST1-FLAG-RFP or GalNAcT-FLAG-HA-RFP). Co-immunoprecipation of ST2-FLAG-GFP from cells transiently transfected with ST1-FLAG-RFP or GalNAcT-FLAG-HA-RFP with antibody against the HA epitope and/or GFP-to-RFP fluorescence energy transfer (FRET) was used to analyze a potential enzyme complex between ST2 and ST1 or GalNAcT. In addition, we have probed the presence of an enzyme−substrate complex between pyrene-labeled GM3 and ST2-FLAG-GFP using pyrene-to-GFP FRET.

MATERIALS AND METHODS

Materials

Murine neuroblastoma x rat dorsal root ganglion F-11 cells were kindly provided by Dr. Glyn Dawson (University of

Chicago, Chicago, IL). A Superscript mouse 15.5-day-old embryo cDNA library in pCMV-Sport 2 vector, Dulbecco's modified Eagle's medium (DMEM), and lipofectamine were obtained from Life Technologies (Gaithersburg, MD). The mammalian FLAG epitope expression system, including pFLAG-CMV-5b expression vector and anti-FLAG BioM2a mouse monoclonal IgG antibody, were from Eastman Kodak Co. (New Haven, CT). The EGFP, EYFP, DsRed vectors, anti-HA rabbit polyclonal IgG, and agarose-linked anti-HA antibody were purchased from Clontech (Palo Alto, CA). Anti-GFP mouse monoclonal IgG antibody, 6-[[*N*-(7-nitrobenz-2-oxa-1,3-diazol-4-yl)amino]hexanoyl]sphingosine (NBD-C6-ceramide), and ER-Tracker Blue-White DPX were from Molecular Probes (Eugene, OR). Donkey polyclonal anti-mouse IgG and anti-rabbit horseradish peroxidase-linked antibody were from Jackson ImmunoResearch (West Grove, PA). Glycopeptidase F (glyco F) and endoglycosidase H (endo H) were purchased from New England Biolabs (Beverly, MA). DEAE-Sephadex A-25, Sephadex LH-20, Triton CF-54, and pyrene-labeled GM3 were obtained from Sigma Chemical Co. (St. Louis, MO). CMP-*N*-[9-^{3}H]-acetylneuraminic acid (33 Ci/mmol) and UDP-*N*-[1-^{3}H]-acetylgalactosamine (50 Ci/mmol) were purchased from New England Nuclear (Boston, MA). Lactosylceramide, GM3, and ganglioside standards were from Matreya (Pleasant Gap, PA). HPTLC plates were from Merck (Darmstadt, Germany). All other chemicals were of analytical grade or higher, and solvents were freshly redistilled before use.

Methods

cDNA Reconstruction and Transfection. As previously described, the cDNAs of ST1, ST2, and GalNAcT were cloned by a PCR-based screening method from a 15.5-day-old mouse embryo cDNA library using oligonucleotide primer combinations as described (*2*, *9*). The cDNAs were first inserted upstream from the FLAG epitope sequence of the pFLAG-5a vector and then recloned into the *Nhe*I and *Sal*I site of the fluorescent protein vector EGFP or EYFP using the forward primer 5′TAGCTAGCAAGATGAGAAGACCCAGC3′ (ST1), 5′TAGCTAGCACACCGAGGCTGCGATGAG3′ (ST2), or 5′TAGCTAGCCATATCAGGATGCGGCTAGAC3′ (GalNAcT) combined with the primer 5′TAGTCGACTTGTCATCGTCGTCCTTGTAATC3′ (FLAG reverse) for amplification of ST1, ST2, or GalNAcT from the pFLAG-5a vector construct. The HA-epitope sequence was introduced between the sequence for FLAG and RFP using the EGFP/YFP vector construct as template and the primer combinations 5′GCTGGTTTAGTGAACCGTCAGATCC3′ (unisense) and 5′TAGTCGACGCGTAGTCTGGGACGTCGTATGGGTACTTGTCATCGTCGTCCTTTGTAAT3′ (HA-FLAG antisense) for the amplification reaction and construction of the DsRed expression vector. Transient and stable transfection of F-11A cells was performed using the lipofectamine procedure following a standard protocol as provided by the manufacturer (Gibco BRL, Gaithersburg, MD).

Cell Culture and Fluorescence Microscopy. Murine neuroblastoma x rat dorsal root ganglion F-11 cells and their derivatives were cultivated in DMEM supplemented with 10% fetal calf serum in a humidified atmosphere containing 5% CO_2 at 37 °C. F-11 cells were separated into single clones and then analyzed for their ganglioside expression. A clone termed F-11A that expresses mainly GM3 was used for stable transfection with the ST2-FLAG-GFP or GalNAcT-FLAG-YFP vector constructs. Cells were fixed with 4% paraformaldehyde in phosphate-buffered saline (PBS) and embedded prior to the analysis by fluorescence microscopy using a Zeiss Axiophot microscope and a Spot CCD camera system. FRET was performed with F-11A cells stably expressing ST2-FLAG-GFP and transiently transfected with ST1-FLAG-HA-RFP or GalNAcT-FLAG-HA-RFP using a filter combination of 425DF60 (excitation) and 600DF15 (emission). The GFP-to-RFP FRET analysis was performed following a previously published protocol that was modified by using a lower wavelength for excitation of GFP in order to exclude cross-contamination by direct excitation of RFP (*10*). For pyrene-to-GFP FRET analysis, ST2-FLAG-GFP expressing F11A cells were incubated with 100 μM GM3 supplemented with 10 μM pyrene-labeled GM3 for 5 h, followed by formaldehyde fixation, embedding, and FRET analysis using a filter combination of 360DF40 (excitation) and 480DF40 (emission). The pyrene-GM3-to-GFP FRET analysis was performed by following a previously published protocol for the analysis of pyrene-GM1-to-NBD FRET (*11*). Pyrene, GFP, or RFP fluorescence was analyzed using a filter combination of 360DF40/425DF60 (pyrene), 425DF60/505DF40 (GFP), or 546DF20/600DF15 (RFP).

Lipid Analysis. Cells were harvested by scraping and subsequent centrifugation at 500*g* for 5 min. The cell pellet was resuspended in 500 μL of water, total lipids were extracted with 5 mL of $CHCl_3/CH_3OH$ (1:1 v/v), and the lipid composition was analyzed following a standard protocol as described (*12*). In brief, acidic lipids were bound to 1 mL of DEAE-Sephadex A-25, and the neutral lipid fraction was washed out with 6 mL of solvent A ($CHCl_3/CH_3OH/H_2O$, 30:60:8 v/v). The acidic lipids were then eluted with 6 mL of 0.4 M sodium acetate in CH_3OH. Phospholipids present in this fraction were removed by alkaline hydrolysis with 0.2 M NaOH for 1 h at 42 °C. The sample was then neutralized with 0.2 mM HCl and desalted by chromatography on a Sephadex LH-20 column. The lipid fraction was evaporated to dryness and redissolved in CH_3OH. Glycolipid samples corresponding to 500 μg of total cellular protein per lane, were analyzed by HPTLC using the solvent system $CHCl_3/CH_3OH$/0.2% $CaCl_2$ (50:45:10 v/v). Gangliosides were specifically stained using the resorcinol−HCl reagent as described (*13*, *14*).

Enzyme Assays. Untransfected F-11A cells and cells expressing ST2-FLAG-GFP or GalNAcT-FLAG-YFP (5×10^6 cells each) were harvested by scraping and resuspended in 100 μL of 10 mM sodium cacodylate buffer (pH 7.0). Aliquots (50 μL) were subjected to lysis with an equal volume of 0.6% Triton CF-54 in 50 mM sodium cacodylate buffer (pH 6.5) and 20 mM $MgCl_2$ (ST1 and ST2 assay buffer, 2-fold concentrated) or 0.6% Triton CF-54 in 50 mM sodium cacodylate buffer (pH 7.2), 20 mM $MnCl_2$, and 4 mg/mL sodium taurocholate (GalNAcT assay buffer, 2-fold concentrated). After lysis for 20 min at 4 °C, the reaction mixtures were centrifuged for 10 min at 14000*g*. Aliquots of the supernatants (50 μL/activity assay) were supplemented with 15 μL of 2.0 mM lactosylceramide (for ST1) or GM3 (for ST2 or GalNAcT) as acceptor lipid and 10 μL of 4.0 mM CMP-*N*-[^{3}H]acetylneuraminic acid (0.5 μCi, ST1 or ST2 assay) or 10 μL of UDP-*N*-[^{3}H]acetylgalactosamine (0.5 μCi,

GalNAcT assay) as donor substrate. The reaction mixtures were brought to a final volume of 100 μL by addition of 25 μL of the appropriate 2-fold concentrated assay buffer and incubated for 3 h at 37 °C. Blank assays were performed with the heat-inactivated enzyme. After the reaction was complete, the radiolabeled glycolipid products were separated from the substrate by chromatography on a Sepadex G-50 column as described (*5*). The radioactivity in the glycolipid product was determined by liquid scintillation counting.

Immunoprecipitation. F-11A cells stably expressing ST2-FLAG-GFP were transiently transfected with the cDNA encoding GalNAcT-FLAG-HA-RFP. Seventy-two hours after transfection, cells (5×10^6) were scraped off and lysed with lysis buffer that was composed of 500 μL of 1% Triton X-100 in 50 mM Tris-HCl (pH 7.2) and 300 mM NaCl, supplemented with 200 μM phenylmethanesulfonyl fluoride and 2 μg/mL aprotinin, leupeptin, and pepstatin for 20 min at 4 °C. The lysed cells were centrifuged for 15 min at 14000*g*, and the supernatant was added to 50 μL of agarose covalently linked to anti-hemagglutinin (αHA) rabbit IgG and preadsorbed to solubilized protein from untransfected F-11A cells. After overnight incubation with gentle rocking at 4 °C, the αHA-agarose was washed five times with the lysis buffer, three times with PBS, and three times with 50 mM Tris-HCl (pH 7.2) before being boiled with 100 μL of SDS sample buffer for SDS−PAGE and immunoblotting using a mouse monoclonal anti-GFP antibody.

Miscellaneous. The amount of protein was determined using a modification of the Folin phenol reagent (Lowry) assay as described (*15*). Protein precipitation was performed following the Wessel and Flügge procedure (*16*), and the protein N-glycosylation was analyzed by digestion with glycopeptidase F or endoglucosaminidase H according to the manufacturer's protocol (New England Biolabs, Beverly, MA). SDS−PAGE was performed using the Laemmli method upon resolubilization and boiling of the precipitated protein in reducing (with β-mercaptoethanol) or nonreducing (without β-mercaptoethanol) sample buffer (*17*). Immunoblotting was carried out as described using the primary antibody and the horseradish peroxidase-coupled secondary antibody at a concentration of 1 or 5 μg/mL, respectively (*18*).

RESULTS

Stable Transfection of F-11A Neuroblastoma Cells with the cDNAs of ST2-FLAG-GFP or GalNAcT-FLAG-YFP Results in the Predominant Expression of b-Series Complex Gangliosides. F-11A cells, a subclone of murine neuroblastoma x dorsal root ganglion F-11 cells, express mainly GM3, whereas GM1 or complex gangliosides are present in this subclone only in trace amount (*8*). Figure 2A shows that stable transfection of F-11A cells with GFP (F-11A-GFP cells) did not change the composition of gangliosides as compared to the untransfected cells (lane 3). As shown in Figure 2B, an in vitro assay with detergent-solubilized enzyme indicated that the absence of GD3 or complex gangliosides in F-11A or F-11A-GFP cells was most likely due to the specific activity of ST2 and GalNAcT being almost 5-fold lower than that of the parental F-11 cells (*8*). Stable transfection of F-11A cells with ST2-FLAG-GFP or GalNAcT-FLAG-YFP, however, shifted the ganglioside expression toward b-series complex gangliosides (Figure 2A, lanes 4 and 5). This was consistent with an almost 20- and 10-fold enhanced specific activity of ST2 or GalNAcT, respectively (Figure 2B). Unexpectedly, stable transfection

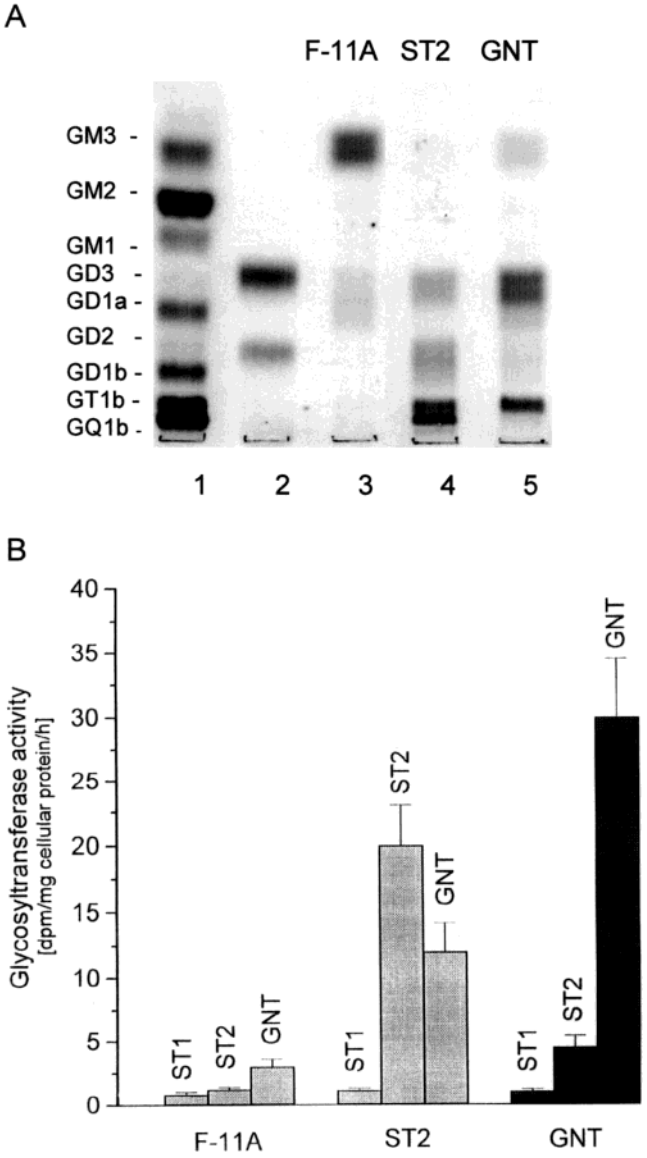

FIGURE 2: Ganglioside expression and glycosyltransferase activities in untransfected and transfected cells. Untransfected or transfected F-11A cells were lysed in organic solvent for ganglioside preparation (A) or with detergent-supplemented buffer for in vitro activity assays (B). (A) Lipids were extracted with solvent A, the neutral lipid fraction was removed by chromatography on DEAE-Sephadex A-25, and phospholipids were eliminated from the acidic lipid fraction by mild alkaline hydrolysis. Gangliosides were separated by HPTLC using the solvent system $CHCl_3/CH_3OH/0.2\%$ $CaCl_2$ (50:45:10 v/v), and individual gangliosides were visualized by staining with the resorcinol−HCl reagent. Each lane shows the ganglioside equivalent of 500 μg of cellular protein: lane 1, ganglioside standard mixture; lane 2, standard GD3 and GD2; lane 3, F-11A cells transfected with GFP; lane 4, F-11A cells transfected with ST2-FLAG-GFP; lane 5, F-11A cells transfected with GalNAcT-FLAG-YFP. (B) Protein was solubilized from cells by lysis with 0.6% Triton CF-54 in buffer, and activity assays were performed with 200 μg of solubilized protein using the appropriate combinations of lipid acceptor and radioactively labeled sugar donor substrates. The product gangliosides were separated by gel filtration on Sephadex G-50, and the transferred radioactivity was determined by liquid scintillation counting. All determinations were made with $N = 5$; bars show averages and standard deviations.

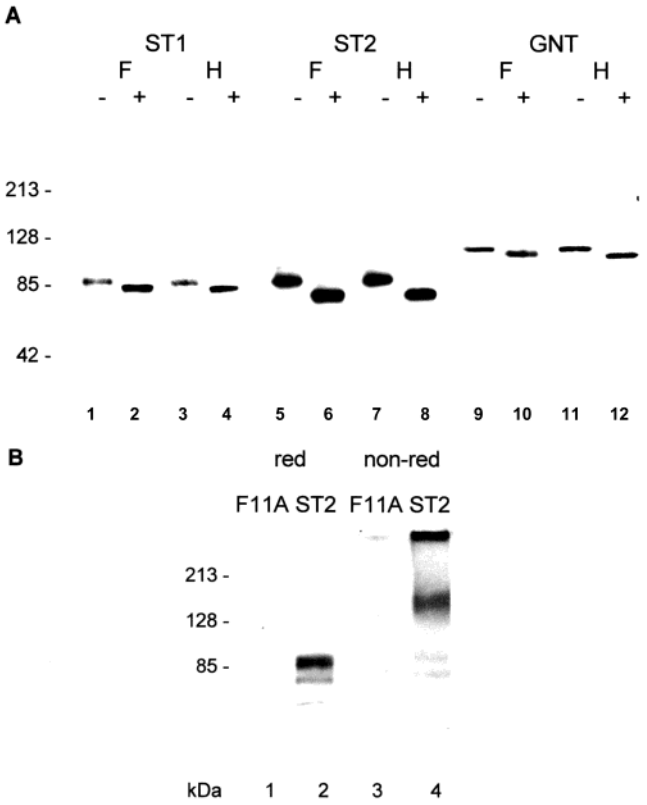

FIGURE 3: Analysis of N-linked oligosaccharide processing and disulfide-stabilized dimerization of glycosyltransferases expressed in F-11A cells. Protein was solubilized from transfected F-11A cells by lysis with 1% Triton X-100 in buffer and then analyzed by incubation with N-linked glycan-specific glycosidases followed by reducing SDS−PAGE (A) or by nonreducing SDS−PAGE (B). (A) Analysis of *N*-glycoprotein processing by incubation with glycopeptidase F (F, cleaves off any type of N-linked oligosaccharide) or endoglucosaminidase H (H, cleaves off only noncomplex oligosacharides of type $Man_5GlcNAc_2$ to $Glc_3Man_9GlcNAc_2$): lanes 1−4, F-11A cells transfected with ST1-FLAG-YFP; lanes 1 and 3; without glyco F or endo H treatment; lanes 2 and 4, with glyco F or endo H treatment, respectively; lanes 5−8, F-11A cells transfected with ST2-FLAG-GFP; lanes 5 and 7, without glyco F or endo H treatment; lanes 6 and 8, with glyco F or endo H treatment, respectively; lanes 9−12, F-11A cells transfected with GalNAcT-FLAG-YFP; lanes 9 and 11, without glyco F or endo H treatment, respectively; lanes 10 and 12, with glyco F or endo H treatment, respectively. (B) Analysis of disulfide-stabilized ST2-FLAG-GFP dimerization by nonreducing SDS−PAGE. Western blots were immunostained using anti-GFP antibody: lanes 1 and 2, reducing SDS−PAGE; lane 1, untransfected F-11A cells; lane 2, F-11A cells transfected with ST2-FLAG-GFP; lanes 3 and 4, nonreducing SDS−PAGE; lane 3, untransfected F-11A cells; lane 4, F-11A cells transfected with ST2-FLAG-GFP.

with either the cDNAs of ST2-FLAG-GFP or GalNAcT-FLAG-YFP also increased the activity of endogenous GalNAcT or ST2, respectively (Figure 2B). The activity of ST1, however, was not affected by stable transfection with ST2 or GalNAcT. Interestingly, the expression of GD3 was higher in GalNAcT-FLAG-HA-RFP than in ST2-FLAG-GFP transfected cells, although the in vitro activity for ST2 was higher in ST2-FLAG-GFP expressing cells than in GalNAcT-FLAG-HA-RFP transfected cells.

Glycosyltransferase Fusion Proteins Are Expressed as ER- and/or Golgi-Localized N-Glycoproteins. Protein from transfected cells was analyzed by SDS−PAGE and immunoblotting using antibodies against GFP that also cross-react with YFP. As shown in Figure 3A, transfection with the cDNAs of ST1-FLAG-YFP (transient), ST2-FLAG-GFP (stable), or GalNAcT-FLAG-YFP (stable) resulted in the expression of fusion proteins with molecular masses of approximately 85 kDa (lane 1 or 3), 85 kDa (lane 5 or 7), or 115 kDa (lane 9 or 11), respectively. The presence of N-linked oligosaccharides was analyzed by digestion with glycopeptidase F (cleaves off all N-linked glycans) or endoglucosaminidase H (specific for noncomplex oligosaccharide chains) prior to SDS−PAGE and immunoblotting. Figure 3A, lanes 1−12, shows that the molecular masses of fusion proteins were each reduced by 3−5 kDa, which is consistent with the removal of two to three noncomplex (endo H-sensitive) glycan chains of about 1.5 kDa each. SDS−PAGE under nonreducing conditions showed that a major portion (about 70−80%) of ST2-FLAG-GFP was immunostained as a protein of about 170 kDa (Figure 3B, lane 4), which is consistent with the molecular mass of a disulfide-linked homodimer. Dimerization, however, could not be found for ST1-FLAG-YFP or GalNAcT-FLAG-YFP (not shown). As shown in Figure 4A, analysis of the subcellular distribution of the glycosyltransferase fusion proteins by fluorescence microscopy revealed that ST2-FLAG-GFP was localized in distinct Golgi compartments, whereas ST1-FLAG-YFP and GalNAcT-FLAG-YFP were broadly distributed in the ER and Golgi. The identification of subcellular compartments was verified by double labeling with ER and Golgi tracker dyes (not shown).

Coexpression of ST2-FLAG-GFP and GalNAcT-FLAG-HA-RFP Results in the Formation of a Golgi-Localized Enzyme Complex. A potential physical association or interaction between the glycosyltransferase fusion proteins was analyzed by transient transfection of ST2-FLAG-GFP expressing F-11A cells (stable) with ST1-FLAG-RFP or GalNAcT-FLAG-HA-RFP vector constructs. As shown in Figure 4B, FRET analysis using the GFP-to-RFP energy transfer revealed that a portion of the Golgi-localized ST2-FLAG-GFP and GalNAcT-FLAG-HA-RFP showed a specific FRET signal. The specificity of this signal was verified by the observation of distinct signals in the green or red fluorescence channel that were not detectable by FRET, thus ruling out fluorescence due to cross-contamination (by RFP excitation) or leakage (by GFP emission). There was no FRET signal detectable upon coexpression of ST2-FLAG-GFP and ST1-FLAG-HA-RFP (Figure 4C). A potential enzyme complex between ST2-FLAG-GFP and GalNAcT-FLAG-HA-RFP was also analyzed by co-immunoprecipitation of ST2 and GalNAcT. ST2-FLAG-GFP expressing cells (stable) were transiently transfected with the cDNA for GalNAcT-FLAG-HA-RFP. The GalNAcT-FLAG-HA-RFP expression product was immunoprecipitated with anti-HA-agarose. As shown in Figure 4D, SDS−PAGE and immunoblot using an antibody against GFP for immunostaining revealed that ST2-FLAG-GFP (lane 3) was co-immunoprecipitated with GalNAcT-FLAG-HA-RFP (lane 4). Immunoprecipitation of ST2-FLAG-GFP or GalNAcT-FLAG-HA-RFP expressing cells without cotransfection was used as a negative control for the precipitation (with anti-HA-agarose) or immunostaining (with anti-GFP-antibody) reaction, respectively. Western blotting of the precipitate did not show any signal for ST2-FLAG-GFP or GalNAcT-FLAG-HA-RFP, thus ruling out nonspecific binding or false-positive staining (lanes 5 and 6).

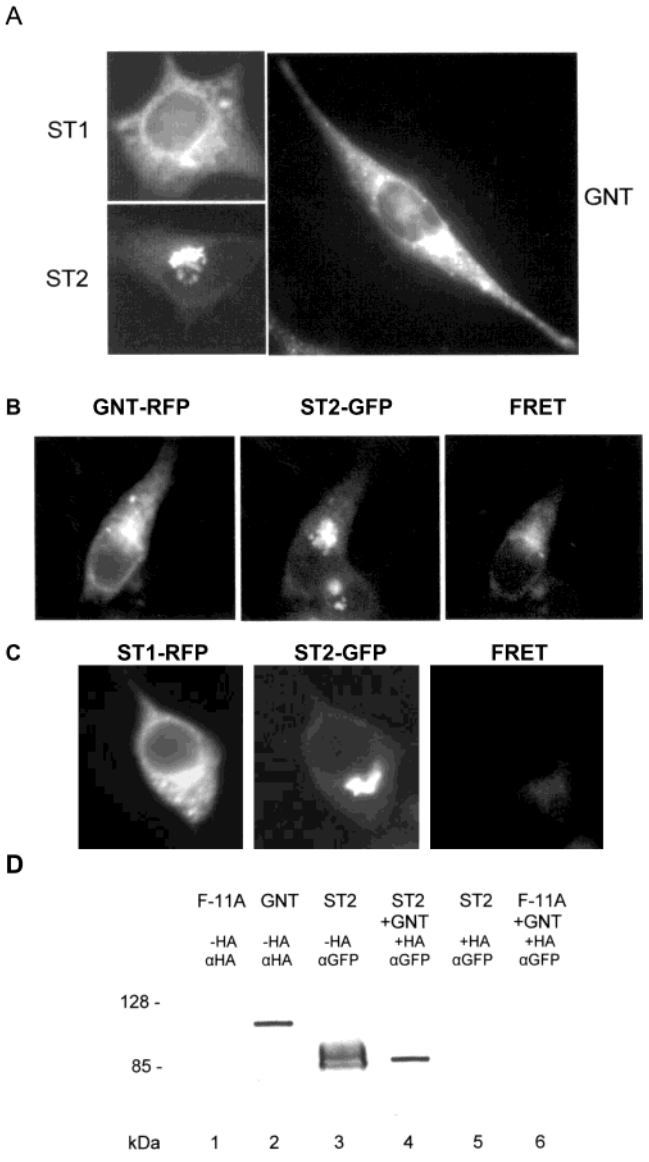

FIGURE 4: Subcellular localization and complex formation of glycosyltransferases. ST1-FLAG-YFP, ST1-FLAG-HA-RFP, ST2-FLAG-GFP, GalNAcT-FLAG-YFP, and GalNAcT-FLAG-HA-RFP were individually expressed in F-11A cells, and the subcellular localization was analyzed by fluorescence microscopy (A). The in situ complex formation was determined by FRET (B, C) or co-immunoprecipitation followed by SDS−PAGE and immunoblotting (D). (A) Transfection of ST1-FLAG-YFP, ST2-FLAG-GFP, or GalNAcT-FLAG-YFP, respectively; **(**B) stable expression of ST2-FLAG-GFP and transient cotransfection of GalNAcT-FLAG-HA-RFP (GNT-RFP); left, GNT-RFP (red fluorescence); middle, ST2-GFP (green fluorescence); right, GFP-to-RFP FRET; (C) stable expression of ST2-FLAG-GFP and transient cotansfection of ST1-FLAG-HA-RFP; left, ST1-RFP (red fluorescence); middle, ST2-GFP (green fluorescence); right, GFP-to-RFP FRET; (D) transient cotransfection of GalNAcT-FLAG-HA-RFP in ST2-FLAG-GFP expressing F-11A cells followed by co-immunoprecipitation of ST2-FLAG-GFP using anti-HA agarose and immunoblotting using anti-HA or anti-GFP for immunostaining; lanes 1−3, immunoblots of cell lysates without prior precipitation with HA-agarose; lane 1, F-11A with anti-HA; lane 2, GalNAcT-FLAG-HA-RFP with anti-HA, lane 3, ST2-FLAG-GFP with anti-GFP; lanes 4−6, immunoblot after immunoprecipation with anti-HA agarose; lane 4, ST2-FLAG-GFP cotransfected with GalNAcT-FLAG-RFP, immunostaining with anti-GFP; lane 5, ST2-FLAG-GFP, immunostaining with anti-GFP; lane 6, GalNAcT-FLAG-RFP, immunostaining with anti-GFP.

ER-Retained ST2-FLAG-GFP Binds to GM3 and Enables the Synthesis of GD3 but Not of BCGs. ST2-FLAG-GFP transfected F-11A cells were incubated for 8 h with various concentrations (20, 50, 100 μM) of GM3. Each sample was supplemented with 10 μM pyrene-labeled GM3 for the analysis of subcellular localization and pyrene-to-GFP FRET. As shown in Figure 5A, panel on top, at 100 μM GM3, a portion of the enzyme was detected in vesicles throughout the cytosol, which decreased with lower concentrations of GM3 (not shown). This result suggests GM3-induced, partial redistribution of ST2-FLAG-GFP by ER retention of the enzyme or by perturbation of the Golgi morphology. The integrity of the Golgi apparatus was verified by monitoring the GFP signal that originated in the portion of Golgi-localized ST2-FLAG-GFP, which was not different from the subcellular distribution of a red fluorescent Golgi tracker dye. A potential complex formation between GM3 and ST2-FLAG-GFP was revealed by pyrene-to-GFP FRET (Figure 5A, panel on bottom). FRET analysis showed a fluorescence signal that was concomitant with the ER distribution of pyrene-labeled GM3. The subcellular localization of ST2-FLAG-GFP was manipulated by incubation of transfected cells with castanospermine, an inhibitor of early *N*-glycoprotein processing, that has been shown to induce redistribution of ST2 to the ER (*2*). As shown in Figure 5B, castanospermine incubation resulted in a distribution of ST2-FLAG-GFP into vesicles throughout the cytosol. The vesicle distribution was similar to that observed upon incubation with pyrene-labeled GM3 (Figure 5A). Figure 5B also shows the HPTLC analysis of gangliosides expressed in ST2-FLAG-GFP transfected cells that were incubated with castanospermine for 72 h. This treatment resulted in the predominant expression of GD3 and GD2 (lane 5). BCGs, however, were only detected in trace amounts.

DISCUSSION

Recently, we introduced a multienzyme kinetic analysis (MEKA) of ganglioside biosynthesis that predicts a rapid transport of ganglioside intermediates between different but contiguous glycosyltransferases (*5*). This transport will be facilitated by the formation of enzyme complexes, the physical evidence of which has recently been shown for the association of GalNAcT and galactosyltransferase II (*4*). A potential complex formation between ST1, ST2, and GalNAcT, the key regulatory enzymes for complex ganglioside biosynthesis, however, has not been analyzed yet. We have carried out this analysis by stable transfection of F-11A cells with cDNAs encoding glycosyltransferases that were C-terminally linked to antigenic epitope tags and different fluorescent proteins. The fusion proteins as expressed in F-11A cells showed a subcellular localization that has previously been described for epitope-tagged glycosyltransferases (*2, 19*). The localization of ST2-FLAG-GFP was confined to the Golgi, whereas ST1-FLAG-YFP and GalNAcT-FLAG-YFP were broadly distributed to ER and Golgi. The fusion proteins were *N*-glycoproteins with endo H-sensitive oligosaccharides, which is consistent with the results obtained with epitope-linked enzymes as reported previously (*2*). The subcellular localization of ST1, however, appeared to be broader than that reported in another study (Golgi), which may indicate a cell- or tissue-specific expression pattern of this enzyme (*20*).

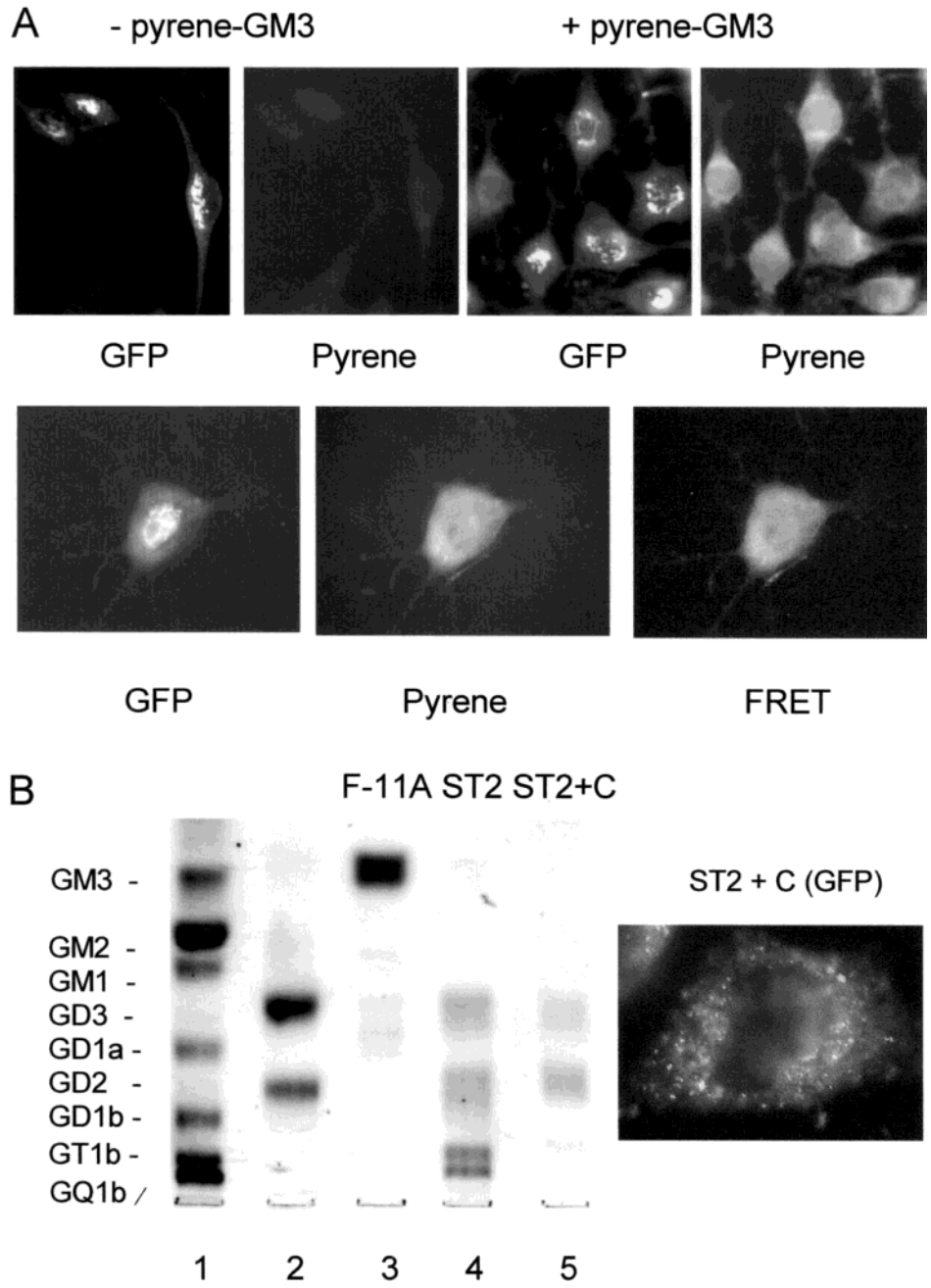

FIGURE 5: ER retention of ST2-FLAG-GFP and complex formation with pyrene-labeled GM3. F-11A cells expressing ST2-FLAG-GFP were incubated with pyrene-labeled GM3 (A) or castanospermine (B), and the effects on subcellular localization and ganglioside biosynthesis were analyzed by fluorescence microscopy or HPTLC. (A) Incubation for 8 h with 10 μM pyrene-labeled GM3: ±GM3, with or without GM3; GFP, green fluorescence of ST2-FLAG-GFP; pyrene, pyrene fluorescence of pyrene-labeled GM3; FRET, pyrene-to-GFP fluorescence energy transfer. (B) Incubation for 72 h with 500 μM castanospermine: lane 1, ganglioside standard mixture; lane 2, standard GD3 and GD2; lane 3, untransfected F-11A cells; lane 4, F-11A cells transfected with ST2-FLAG-GFP; lane 5, same as in lane 4, but after incubation with castanospermine.

HPTLC analysis of ganglioside expression in ST2-FLAG-GFP or GalNAcT-FLAG-YFP transfected cells revealed a ganglioside composition that was completely unexpected. We expected that the transfected cells expressed predominantly GD3 (transfection with ST2) or a-series complex gangliosides (transfection with GalNAcT) and only trace amounts of BCGs as predicted from the low activity of endogenous GalNAcT or ST2 in the host cell line, respectively. The transfected cells, however, showed a predominant expression of BCGs, suggesting that the expressed enzymes enhance the activity of endogenous glycosyltransferases. This assumption was confirmed by in vitro enzyme assays revealing a 5-fold enhanced activity of endogenous GalNAcT by stable transfection with ST2-FLAG-GFP and a 3-fold enhanced activity of endogenous ST2 by stable transfection with GalNAcT-FLAG-YFP. The ganglioside pattern or the enzyme activities were not changed by stable transfection of F-11A cells with GFP alone, indicating that neither the expression of GFP nor the transfection method affected ganglioside biosynthesis. These observations suggest that F-11A cells, despite showing low activities of endogenous ST2 and GalNAcT, may enhance these activities by transfection with the glycosyltransferase catalyzing the previous or subsequent reaction in the ganglioside biosynthetic

pathway. This activation reaction is specific for ST2 or GalNAcT as concluded from the observation that the activity of ST1 was not enhanced by transfection of F-11A cells with ST2 or GalNAcT. We hypothesize that, upon transfection of F-11A cells with the cDNAs of ST2 or GalNAcT, the expressed enzymes formed a complex with endogenous GalNAcT or ST2, respectively, resulting in activation of the associated enzymes. The activity of endogenous ST1, however, appeared not to be affected by stable transfection with ST2 or GalNAcT, suggesting that the entry reaction of ganglioside biosynthesis was not part of the activation process.

Formation of a complex between ST2 and GalNAcT was analyzed upon transient transfection of ST2-FLAG-GFP expressing cells with GalNAcT-FLAG-HA-RFP. The analysis was based on co-immunoprecipitation studies and FRET fluorescence microscopy. Western blot analysis of an immunoprecipitate obtained with an HA-specific antibody showed the presence of ST2-FLAG-GFP that was immunostained with an antibody against GFP. This result indicates that ST2-FLAG-GFP was co-immunoprecipitated due to physical association to GalNAcT-FLAG-HA-RFP. GFP-to-RFP FRET showed that the formation of the ST2-GalNAcT complex is confined to distinct regions within the Golgi. The specificity of the FRET signal was validated by the observation that the GFP and RFP fluorescence showed additional signals that were not detected using the filter combination for FRET. The FRET signal was not visible upon transient transfection of ST2-FLAG-GFP expressing cells with the ST1-FLAG-RFP vector, indicating that FRET was absent if the glycosyltransferase fusion proteins were colocalized in the Golgi but not physically associated in an enzyme complex. This specificity is thus consistent with the observation that ST2 and GalNAcT were activated when simultaneously expressed, whereas the activity of ST1 remained unaffected.

Recently, we have demonstrated that ST2 is retained within the ER if the processing of N-linked oligosaccharides is impaired by incubation of transfected cells with castanospermine, an inhibitor of the trimming glucosidases I and II (*2*). ER retention was found to result from a failure of the nonprocessed enzyme to bind to calnexin, a chaperone that participates in *N*-glycan-assisted protein folding. We incubated ST2-FLAG-GFP transfected cells with castanospermine and analyzed the ganglioside expression. ST2-FLAG-GFP was retained within the ER, indicating that the fusion protein was subjected to the same posttranslational protein sorting mechanism as the epitope-tagged enzyme. The castanospermine-incubated cells expressed mainly GD3 and GD2, suggesting that the ER-retained form of ST2 may associate with GM3 that has been synthesized within the ER or redistributed to this compartment via Golgi-to-ER membrane transport. GM3 was converted to GD3 and then to GD2, most likely due to the activity of the ER-resident portion of endogenous GalNAcT. A subsequent conversion to BCGs, however, was only found in trace amount, indicating that the overall substrate flow within the ganglioside biosynthetic pathway is controlled by the subcellular localization and further association of particular glycosyltransferases downstream of GalNAcT.

A potential binding of the entry substrate GM3 to ST2-FLAG-GFP was analyzed by incubation of transfected cells with pyrene-labeled GM3 and pyrene-to-GFP FRET. Strong FRET signals were found in vesicles throughout the cytosol, indicating that GM3 may form a stable complex with ST2 in the ER, which is then transported to the Golgi. In the Golgi, a subsequent conversion of GM3 to GD3 is facilitated by prior association with GalNAcT, which is consistent with the observation that the two enzymes were activated as shown by in vitro enzyme assays. The assumption that GM3 and ST2 form a stable complex is also corroborated by previous studies showing that ST2 could be affinity-purified with immobilized GM3 and that the formation of an enzyme−substrate complex stabilized in vitro translated ST2 (*21*, *22*). The significantly weaker FRET signal in the Golgi suggests, however, that the half-life of the ST2−GM3 complex is short in this compartment.

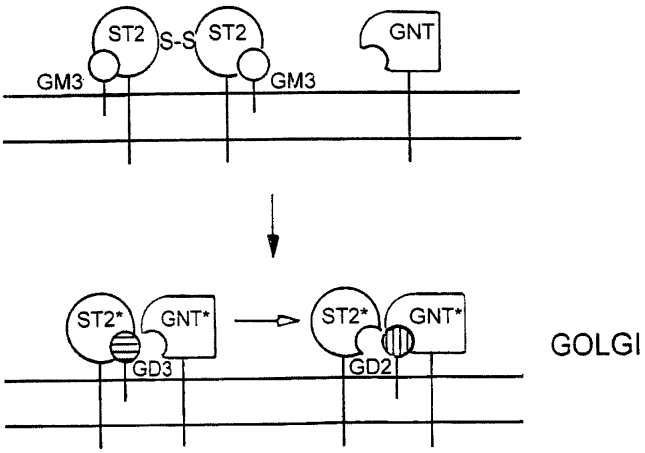

FIGURE 6: Model of ganglioside biosynthesis regulation by subcellular localization and complex formation of ST2 and GalNAcT. In the ER or Golgi, ST2 is dimerized by disulfide linkage, which stabilizes complex formation with GM3. ST2 and GalNAcT are transported to the Golgi where they form a heterodimer with mutual enzyme activation. In this heterodimer, ST2 converts GM3 to GD3 and channels it to the active site of GalNAcT. GalNAcT converts GD3 to GD2; further glycosylation depends on the activity, subcellular localization, or complex formation with additional glycosyltransferases. *, activated enzymes.

Figure 6 shows a model that integrates posttranslational modification and subcellular localization of ST2 and GalNAcT into the regulation of ganglioside biosynthesis in F-11A cells. GM3 is bound to ST2, the dimerization of which via disulfide linkage may be facilitated due to the formation of a cooperative enzyme−substrate complex. Our results and the postulated model are consistent with recent studies that have shown a disulfide-stabilized formation of ST2 dimers (*4*). Disulfide bonds have also been reported to stabilize homodimers of GalNAcT (*23*, *24*); however, these complexes were not shown in our system. In F-11A cells, due to the low endogenous ST2 and GalNAcT activity, we conclude that enhanced expression of at least one of the two enzymes is the prerequisite for the formation of an enzyme complex with enhanced activity. Hence, further conversion of GM3 to GD3 will be facilitated by the association of ST2-GM3 with GalNAcT upon transient transfection with the respective cDNA construct. The absence of GM1 or a-series complex gangliosides in untransfected and transfected F-11A cells is consistent with the assumption that endogenous or transfected GalNAcT fails to convert GM3 without activation by complex formation with ST2. As reported previously, as-

sociation of GalNAcT with GalT2, and probably other glycosyltransferases in the Golgi, will then entail the biosynthesis of b-series complex gangliosides (*4*, *25*). The specific nature and composition of this multienzyme complex may also account for the differences within the regulation of individual gangliosides in transfected F-11A cells. In particular, the expression of GD3, which is more robust in GalNAcT-FLAG-HA-RFP than in ST2-FLAG-GFP transfected cells, appears to be paradoxical in light of the in vitro activities of these enzymes. Although this observation remains unexplained, it is very likely that in vivo activities are modulated by the recruitment of additional glycosyltransferases (e.g., GalT2) in a larger enzyme complex, which may involve regulatory effects that are not completely seen with the in vitro activities. For example, the in vivo activity of GalNAcT may be more enhanced in ST2-FLAG-GFP transfected than in GalNAcT-FLAG-HA-RFP expressing cells. This would explain a higher consumption of GD3 and the expression of more BCGs. However, these specific differences between ST2-FLAG-GFP and GalNAcT-FLAG-HA-RFP expressing cells will be the subject of our future studies on enzyme complex formation and mutual activation of glycosyltransferases in ganglioside biosynthesis.

In conclusion, our observations are consistent with multienzyme kinetic analysis (MEKA) that predicts the dependence of individual ganglioside levels on the activity of the converting enzyme rather than on the enzyme that catalyzes the synthesis of a particular ganglioside (*5*). Our model for the regulation of ganglioside biosynthesis by subcellular localization and complex formation of glycosyltransferases is also consistent with experimental observations from previous studies that suggested enzyme complexes comprised of glycosyltransferases (*4*, *6*, *7*, *25*). To date, it is not clear how many glycosyltransferases are associated within a Golgi-localized multienzyme complex. Formation of enzyme complexes and mutual activation of glycosyltransferases, however, would explain the observation that, in early mouse brain development and during early in vitro neuronal differentiation of P19 cells, a-series complex gangliosides are only detectable in trace amounts despite ample expression of GalNAcT (*3*, *8*, *26*). In further studies, we will investigate which glycosyltransferases participate in a Golgi-localized multienzyme complex and how its formation is mediated and regulated. We will also analyze the regulation of the complex formation and its significance for ganglioside biosynthesis, in particular, for switching from simple to complex, and then from a- to b-series gangliosides as observed during neuronal development.

ACKNOWLEDGMENT

The authors thank Drs. Boris Baibakov (currently at Johns Hopkins University, Baltimore, MD), Sean Liour, and Stacey Kraemer (Medical College of Georgia) for critical discussions and the IMMAG Imaging Core Facility under the supervision of Dr. Steven Vogel (Medical College of Georgia) for assistance with fluorescence microscopy and FRET.

REFERENCES

1. Svennerholm, L. (1963) *J. Neurochem. 10*, 613−623.
2. Bieberich, E., Tencomnao, T., Kapitonov, D., and Yu, R. K. (2000) *J. Neurochem. 74*, 2359−2364.
3. Yu, R. K. (1994) *Prog. Brain Res. 101*, 31−44.
4. Giraudo, C. G., Daniotti, J. L., and Maccioni, H. J. F. (2001) *Proc. Natl. Acad. Sci. U.S.A. 98*, 1625−1630.
5. Bieberich, E., and Yu, R. K. (1999) *Biochim. Biophys. Acta 1432*, 113−124.
6. Roseman, S. (1970) *Chem. Phys. Lipids 5*, 270−279.
7. Chen, C., Ma, J., Lazic, A., Backovic, M., and Colley, K. J. (2000) *J. Biol. Chem. 275*, 13819−13826.
8. Bieberich, E., MacKinnon, S., Silva, J., and Yu, R. K. (2001) *J. Biol. Chem. 276*, 44396−44404.
9. Kapitonov, D., Bieberich, E., and Yu, R. K. (1999) *Glycoconjugate J. 16*, 337−350.
10. Mas, P., Devlin, P. F., Panda, S., and Kay, S. A. (2000) *Nature 408*, 207−211.
11. McCann, J. A., Mertz, J. A., Czworkowski, J., and Picking, W. D. (1997) *Biochemistry 36*, 169−178.
12. Freischutz, B., Tokuda, A., Ariga, T., Bermudez, A. J., and Yu, R. K. (1997) *J. Neurochem. 68*, 2070−2078.
13. Svennerholm, L. (1957) *Biochim. Biophys. Acta 24*, 604−611.
14. Yu, R. K., and Ariga, T. (2000) *Methods Enzymol. 312*, 115−134.
15. Wang, C.-S., and Smith, R. L. (1975) *Anal. Biochem. 63*, 414−417.
16. Wessel, D., and Flugge, U. I. (1984) *Anal. Biochem. 138*, 141−143.
17. Laemmli, U. K. (1970) *Nature 227*, 680−685.
18. Gershoni, J. M., and Palade, G. E. (1983) *Anal. Biochem. 13*, 1−15.
19. Daniotti, J. L., Martina, J. A., Giraudo, C. G., Zurita, A. R., and Maccioni, H. J. F. (2000) *J. Neurochem. 74*, 1711−1720.
20. Stern, C. A., Braverman, T. R., and Tiemeyer, M. (2000) *Glycobiology 10*, 365−374.
21. Bieberich, E., Kapitonov, D., Tencomnao, T., and Yu, R. K. (2000b) *Anal. Biochem. 287*, 294−298.
22. Gu, X. B., Gu, T. J., and Yu, R. K. (1990) *Biochem. Biophys. Res. Commun. 166*, 387−393.
23. Jaskiewicz, E., Zhu, G., Bassi, R., Darling, D. S., and Young, W. W., Jr. (1996) *J. Biol. Chem. 271*, 26398−26403.
24. Li, J., Yen, T. Y., Allende, M. L., Joshi, R. K., Cai, J., Pierce, W. M., Jaskiewicz, E., Darling, D. S., Macher, B. A., and Young, W. W., Jr. (2000) *J. Biol. Chem. 275*, 41476−41486.
25. Van Meer, G. (2001) *Proc. Natl. Acad. Sci. U. S.A. 98*, 1321−1323.
26. Liour, S. S., Kapitonov, D., and Yu, R. K. (2000) *J. Neurosci. Res. 62*, 363−373.

BI0259958